# Structural, electronic, and elastic properties of K-As compounds: a first principles study

**Havva Bogaz Ozisik · Kemal Colakoglu · Engin Deligoz · Haci Ozisik**

**Abstract** First-principle calculations are performed to investigate the structural, elastic and electronic properties of K-As compounds (KAs in NaP, LiAs and AuCu-type structures, $KAs_2$ in $MgCu_2$-type structure, $K_3As$ in $Na_3As$, $Cu_3P$ and $Li_3Bi$-type structures, and $K_5As_4$ in $A_5B_4$-type structure). The lattice parameters, cohesive energy, formation energy, bulk modulus, and the first derivative of bulk modulus (to fit to the Murnaghan's equation of state) of the considered structures are calculated and reasonable agreement is obtained, and the phase transition pressure is also predicted. The repeated calculations on the electronic band structures and the related partial density of states are also given. The calculated second-order elastic constants based on the stress-strain method and the other related quantities such as Young's modulus, shear modulus, Poisson's ratio, sound velocities, Debye temperature, and shear anisotropy factors for considered structures are presented, and trends are discussed.

**Keywords** Alkaline metal pnictides · Elastic properties · Electronic properties · K-As compounds

## Introduction

Alkali metal pnictides are a member of the family of Zintl phase which has drawn the attention of scientists in inorganic research for many years [1, 2]. These materials show different physical and chemical properties depending on the structure and chemical composition [2–4]. For different stoichiometry and structures, they possess a band gap range from 0.1 eV up to 2.5 eV. This important property is used in thin film and photocathode application [5, 6]. Some alkali pnictides are also used in crystal growth techniques [7–9].

There are many studies on alkali pnictides, but most of them are on the compounds of the alkali metals with Sb and Bi elements. Only a few recent theoretical or experimental works on K-As compounds have been reported [10–20]. Therefore, we believe that many theoretical and experimental research efforts are needed to explore their various physical properties in different crystal structures and different stoichiometries. For these purposes, in an early work, the structural parameters, melting points, standard enthalpies, and entropies of formation of the synthesized K-As compounds were investigated in orthorhombic NaP, hexagonal $Na_3As$, and $Cu_3P$ structures [10]. The crystal structure of $K_3As$ using the x-ray method was analyzed by Brauer and Zintl [11]. The crystal structure of $K_3As$ in $Cu_3P$-type structure was studied by Mansmann [12]. Emmerling and Röhr characterized KAs in NaP structure via single crystal x-ray studies [13]. The structure of $K_5As_4$ from single-crystal X-ray diffraction was determined by Gascoin and Sevov [14]. Hönle et al. synthesized NaP-type KAs compound and examined structural parameters [15]. Emmerling investigated the KAs compound in NaP-type and $K_5As_4$ structures by X-ray diffraction methods [16]. In an early work, the enthalpy and entropy of formation for KAs, $K_3As$, and $K_5As_4$ were determined experimentally [17]. The phase diagram of the K-As system depending on temperature and composition were studied by Dorn et al. [18]. Theoretically, less attention has been paid to these compounds and there are only a few works on the half metallic ferromagnetism for KAs in Zinc Blende [19] and rock salt structure [20].

H. B. Ozisik · K. Colakoglu
Faculty of Science, Physics Department, Gazi University,
06500 Ankara, Turkey

H. B. Ozisik (✉) · E. Deligoz · H. Ozisik
Faculty of Arts and Science, Physics Department, Aksaray University,
68100 Aksaray, Turkey
e-mail: havvabogaz@gmail.com

To our knowledge, despite these efforts, the information on the structural phase transitions, electronic properties and elastic properties, which are the important bulk properties, is not available for K-As compounds. Here, we aim to fill this gap by investigating the structural, electronic, and elastic properties of K-As compounds for different stoichiometries and structures (KAs in NaP, LiAs and AuCu-type structures, $KAs_2$ in $MgCu_2$-type structure, $K_3As$ in $Na_3As$, $Cu_3P$ and $Li_3Bi$-type structures, and $K_5As_4$ in $A_5B_4$-type structure (see Fig. 1)) in detail and interpret the salient results. Detailed crystallographic parameters of the considered structures are given in Table 1. The considered structures in Table 1 are the most probable ones and they are chosen by taking into account their phase diagram and the similar structures of other alkali pnictides. The layout of this paper is as follows: The method of calculation is given in Sect. 2. The results and overall conclusion are presented and discussed in Sects. 3 and 4, respectively.

## Method of calculation

All calculations have been carried out using the Vienna ab-initio simulation package (VASP) [21–24] based on the density functional theory (DFT). For the exchange and correlation terms in the electron- electron interaction, Perdew-Burke-Ernzerhof (PBE) [25] was used within the generalized gradient approximation (GGA). The electron-ion interaction was considered in the form of the projector-augmented-wave (PAW) method [22, 26] with plane wave up to energy of 450 eV. The k-mesh values determined by choosing k-point separation 0.02 Å$^{-1}$ given in Table 1 were found sufficient for the total energy calculations. Structural optimization was performed for each structure for all lattice constants, angles, and internal atomic coordinates until the

difference in total energy and the maximum force was within 1.0 x 10$^{-6}$ eV and 1.0 x 10$^{-4}$ eV/Å, respectively. For a given volume of the unit cell, the lattice parameters are determined in such a way that the total energy becomes a minimum. The data of total energy versus volume were fitted using the Murnaghan's equation of state (eos) [27]. Besides the equilibrium volume, this fitting procedure gives the minimum value of the total energy $E$, the isothermal bulk modulus $B$ and its pressure derivative $B'$ at the equilibrium state.

## Results and discussion

### Structural properties

First, we have optimized the volume of the cell and the ionic positions of atoms. The obtained parameters were used to calculate other physical properties. The calculated atomic positions and lattice parameters are listed in Tables 1 and 2 along with the available works for comparison.

The crystal total energy is calculated for different values of lattice constants, and fitted in terms of Murnaghan's eos [27] (See Fig. 2). As can be seen from Fig. 2, the NaP-type and $Cu_3P$-type are the most stable phases for KAs and $K_3As$ compounds, respectively. It can be seen from the data in Table 2 that the calculated lattice parameters are in agreement with experimental ones (around 2%) except for KAs compound in NaP structure. The calculated lattice constant a-axis is overestimated about 3% and b-axis is underestimated 4.5% from the Ref. [16] for KAs compound in NaP structure, respectively. The calculated bulk modulus, and its pressure derivatives are listed in Table 2 and they are in good agreement with experimental ones.



Fig. 1 The crystal structures models of K-As compounds in (a) NaP, (b) LiAs, (c) AuCu, (d) $MgCu_2$ (e) $Na_3As$, (f) $Cu_3P$, (g) $Li_3Bi$ and (h) $A_5B_4$ structures
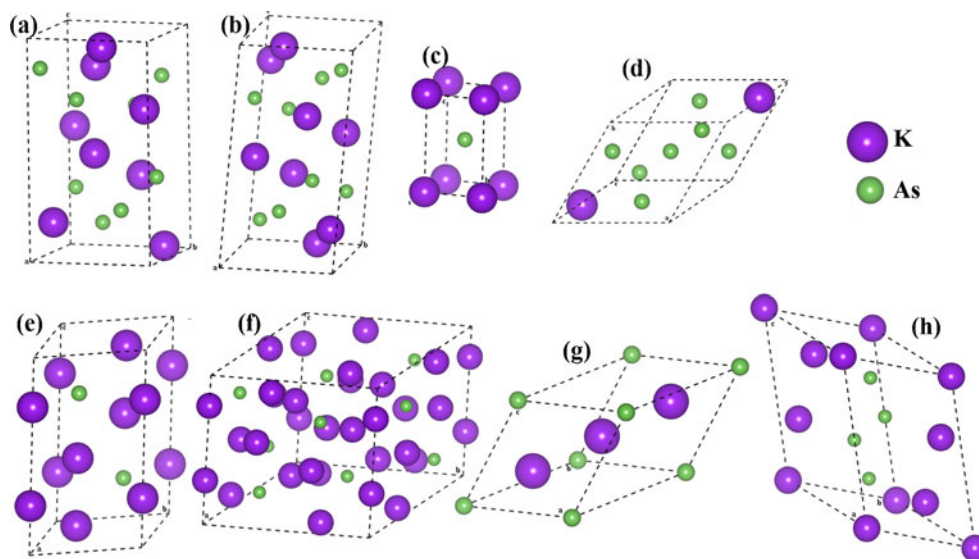
**Table 1** Crystallographic data for considered structures of K-As compounds and the calculated atomic positions after local optimizations on the *ab initio* level (GGA-PBE)

| Compound | Space group (number) | Prototype | Atom | Site | GGA-PBE | k-grid mesh |
|---|---|---|---|---|---|---|
| KAs | P2$_1$2$_1$2$_1$ (19) Orthorhombic | NaP | K$_1$ | 4a (x$_1$, y$_1$, z$_1$) | 4a (0.3950, 0.9158, 0.0394) | 8×8×5 |
| | | | K$_2$ | 4a (x$_2$, y$_2$, z$_2$) | 4a (0.1432, 0.6498, 0.3318) | |
| | | | As$_1$ | 4a (x$_3$, y$_3$, z$_3$) | 4a (0.3156, 0.1574, 0.2831) | |
| | | | As$_2$ | 4a (x$_4$, y$_4$, z$_4$) | 4a (0.4309, 0.4176, 0.1388) | |
| KAs | P2$_1$/c (14) Monoclinic | LiAs | K$_1$ | 4e (x$_1$, y$_1$, z$_1$) | 4e (0.2074, 0.3974, 0.3317) | 8×8×5 |
| | | | K$_2$ | 4e (x$_2$, y$_2$, z$_2$) | 4e (0.2490, 0.6673, 0.0303) | |
| | | | As$_1$ | 4e (x$_3$, y$_3$, z$_3$) | 4e (0.3365, 0.9026, 0.2806) | |
| | | | As$_2$ | 4e (x$_4$, y$_4$, z$_4$) | 4e (0.3470, 0.1679, 0.1368) | |
| KAs | P4/mmm (123) Tetragonal | AuCu | K | 1a (0, 0, 0) | 1a (0, 0, 0) | 8×8×11 |
| | | | As | 1 d(1/2, 1/2, 1/2) | 1d (0.5, 0.5, 0.5) | |
| KAs$_2$ | Fd-3 m (227) Cubic | MgCu$_2$ | K | 8a (1/8, 1/8, 1/8) | 8a (0.125, 0.125, 0.125) | 6×6×6 |
| | | | As | 16 d (1/2, 1/2, 1/2) | 16 d (0.5, 0.5, 0.5) | |
| K$_3$As | P6$_3$/mmc (194) Hexagonal | Na$_3$As | K$_1$ | 2b (0, 0, 1/4) | 2b (0, 0, 0.25) | 10×10×6 |
| | | | K$_2$ | 4f (1/3, 2/3, z$_1$) | 4f (0.3333, 0.6667, 0.5787) | |
| | | | As | 2c (1/3, 2/3, 1/4) | 2c (0.3333, 0.6667, 0.25) | |
| K$_3$As | Fm-3 m (225) Cubic | Li$_3$Bi | K$_1$ | 4b (1/2, 1/2, 1/2) | 4b (0.5, 0.5, 0.5) | 7×7×7 |
| | | | K$_2$ | 8c (1/4, 1/4, 1/4) | 8c (0.25, 0.25, 0.25) | |
| | | | As | 4a (0, 0, 0) | 4a (0, 0, 0) | |
| K$_3$As | P63cm (185) Hexagonal | Cu$_3$P | K$_1$ | 2a (0, 0, z$_1$) | 2a (0, 0, 0.2955) | 6×6×6 |
| | | | K$_2$ | 4b (1/3, 2/3, z$_2$) | 4b (0.3333, 0.6667, 0.2189) | |
| | | | K$_3$ | 6c (x$_1$, 0, z$_3$) | 6c (0.2945, 0, 0.5760) | |
| | | | K$_4$ | 6c (x$_2$, 0, z$_4$) | 6c (0.3677, 0, 0.9161) | |
| | | | As | 6c (x$_3$, 0, z$_5$) | 6c (0.3292, 0, 0.2455) | |
| K$_5$As$_4$ | C2/m (12) Monoclinic | A$_5$B$_4$ | K$_1$ | 4i (x$_1$, 0, z$_1$) | 4i (0.1067, 0, 0.3974) | 6×6×6 |
| | | | K$_2$ | 4i (x$_2$, 0, z$_2$) | 4i (0.7554, 0, 0.1704) | |
| | | | K$_3$ | 2a (0, 0, 0) | 2a (0, 0, 0) | |
| | | | As$_1$ | 4i (x$_3$, 0, z$_3$) | 4i (0.4562, 0, 0.1894) | |
| | | | As$_2$ | 4i (x$_4$, 0, z$_4$) | 4i (0.4047, 0, 0.3943) | |

As a fundamental physical property, the bulk modulus of solids provides valuable information including the average bond strengths of atoms for the given crystals [28]. In the present case, the largest value of bulk modulus (44.5 GPa) is obtained for MgCu$_2$ phase, and it implies that this structure is the least compressible one among the others.

The cohesive energy is known as a measure of the strength of the forces, which bind atoms together in the solid state. In this context, the cohesive energies of K-As compounds are calculated in the considered structures using the following relations:

$$E_{coh}^{K_xAs_y} = E_{total}^{K_xAs_y} - \left[ xE_{atom}^K + yE_{atom}^{As} \right], \quad (1)$$

where $x$ and $y$ refer to the numbers of K and As atoms in a formula unit, respectively. $E_{total}^{K_xAs_y}$ is the total energy (in formula unit) of the compound at the equilibrium lattice

constant and $E_{atom}^K$ and $E_{atom}^{As}$ are the atomic energies of the pure constituents calculated using a large cutoff $r_{max}=15$ Å (free atom). Also from the total energy of the compound and the constituent elemental solids (BCC W-type (Im-3 m, #229, A2) for Potassium and rhombohedral $\alpha$-As-type (R-3 m, #166, A7) for Arsenic element), one can obtain the formation energy using the relation

$$E_{form}^{K_xAs_y} = E_{total}^{K_xAs_y} - \left[ xE_{solid}^K + yE_{solid}^{As} \right]. \quad (2)$$

The calculated cohesive and formation energies are listed in Table 2 and they are in agreement with the values of ref [17]. These results imply that present compounds possesses the negative formation energy and can easily been synthesized in various stable phases. The ranking order of cohesive energy and the formation energy follow a similar trend. The formation energy and cohesive energy of NaP, MgCu$_2$,

**Table 2** The calculated equilibrium lattice parameters ($a$, $b$, and $c$ in Å), bulk modules ($B$ in $GPa$), and its pressure derivatives ($B'$), band gap ($E_g$ in $eV$), cohesive energy ($E_{coh}$ in eV/f.u.), and formation enthalpy ($\Delta H_f$ in eV/f.u.)

| Compound | Prototype | a | b | c | β (°) | B (eos) | B′ | E_g | E_coh | ΔH_f |
|---|---|---|---|---|---|---|---|---|---|---|
| KAs | NaP | 6.8264 | 6.5776 | 11.7990 | | 24.9 | 4.287 | 0.654 | -6.587 | -0.906 |
| | | 6.676[a] | 6.426[a] | 11.584[a] | | | | | | -1.188[g] |
| | | 6.681[b] | 6.425[b] | 11.602[b] | | | | | | |
| | | 6.617[c] | 6.888[c] | 11.973[c] | | | | | | |
| KAs | LiAs | 6.8277 | 6.5433 | 12.7410 | 113.9 | 25.8 | 4.164 | 0.904 | -6.581 | -0.900 |
| KAs | AuCu | 4.4806 | | 5.2137 | | 29.9 | 4.427 | | -5.880 | -0.199 |
| KAs₂ | MgCu₂ | 8.3589 | | | | 44.5 | 4.264 | | -10.989 | -0.654 |
| | | | | | | | | | | -1.340[g] |
| K₃As | Na₃As | 5.8828 | | 10.4230 | | 13.0 | 4.097 | 0.092 | -9.036 | -1.301 |
| | | 5.794[d] | | 10.243[d] | | | | | | -2.104[g] |
| K₃As | Li₃Bi | 8.2338 | | | | 13.7 | 4.304 | 0.468 | -8.834 | -1.099 |
| K₃As | Cu₃P | 10.1952 | | 10.4139 | | 13.0 | 4.242 | 0.080 | -9.044 | -1.309 |
| | | 10.015[e] | | 10.222[e] | | | | | | |
| K₅As₄ | A₅B₄ | 11.8761 | 5.2504 | 10.5376 | 112.07 | 22.7 | 4.4 | | -27.705 | -3.954 |
| | | 11.582[c] | 5.218[c] | 10.387[c] | 113.440[c] | | | | | -5.192[g] |
| | | 11.592[f] | 5.2114[f] | 10.383[f] | 113.42[f] | | | | | |

[a] Exp. Ref [10]

[b] Exp. Ref [15]

[c] Exp. Ref [16]

[d] Exp. Ref [11]

[e] Exp. Ref [12]

[f] Exp. Ref [14]

[g] Exp. Ref [17]
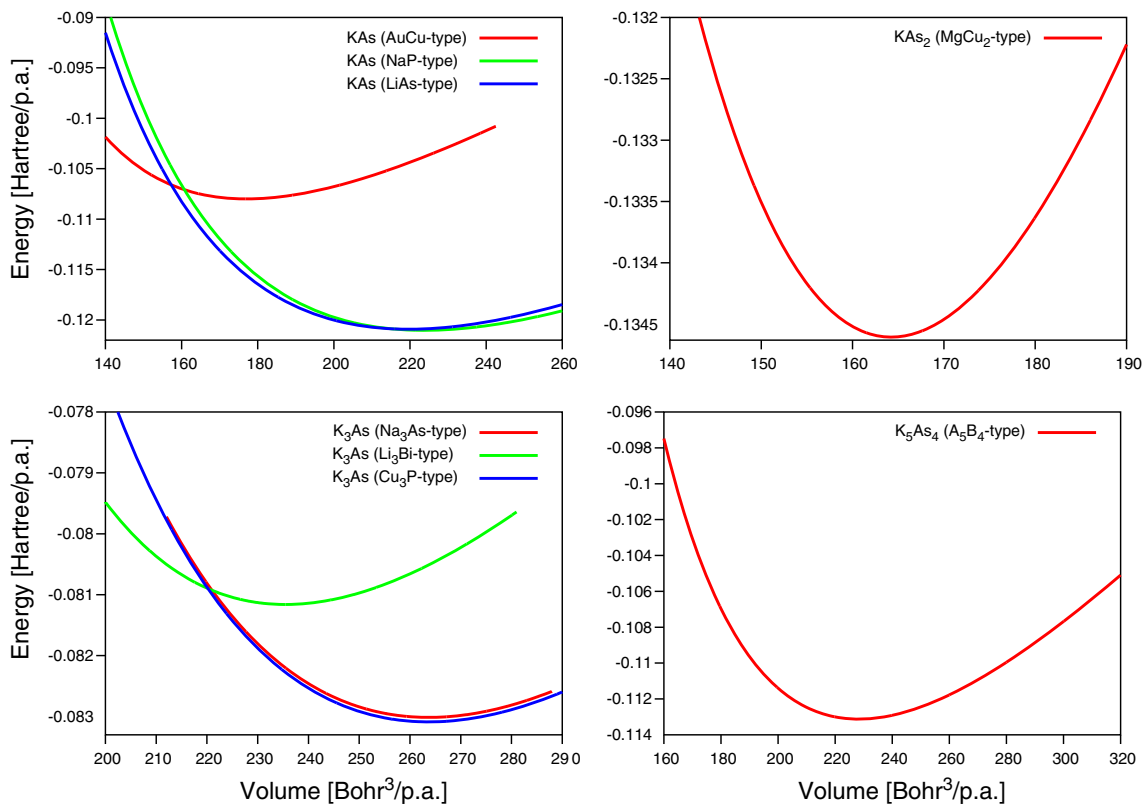


**Fig. 2** The calculated energy–volume curves of the considered phases of K-As compounds

**Fig. 3** Estimation of phase transition pressure from Na$_3$As to Li$_3$Bi phase for K$_3$As compound (Same method is used for the other transitions)
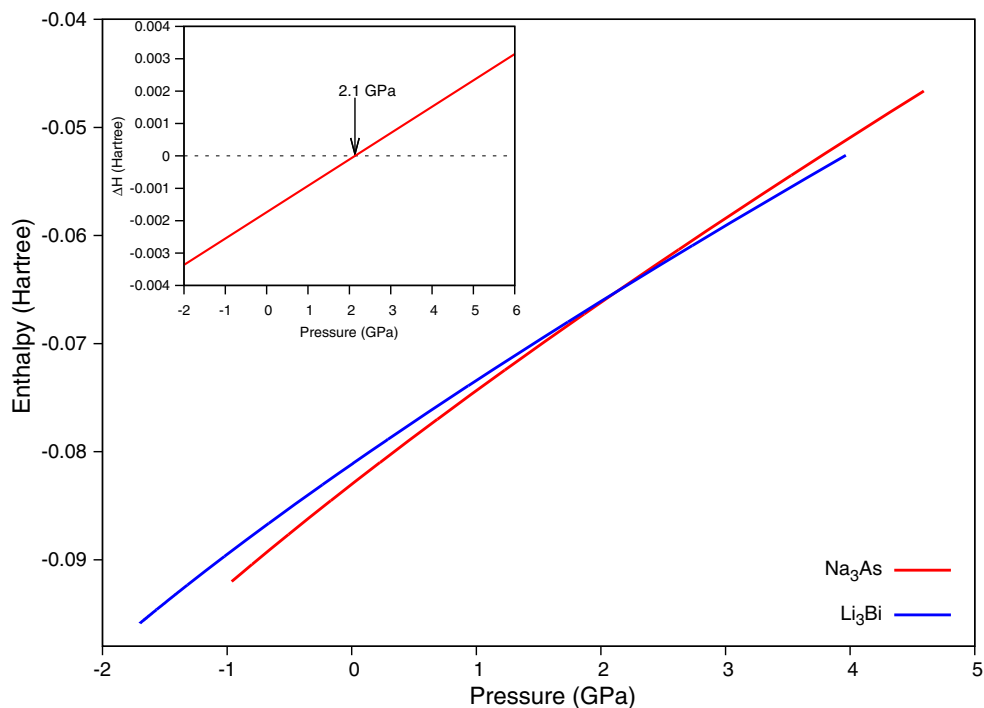
Cu$_3$P, and A$_5$B$_4$ phases are relatively higher than the other types of stoichiometries. It is seen from Table 2 that the NaP and LiAs have almost the same formation energy and similarly, the formation energy for Na$_3$As and Cu$_3$P phases are almost the same. The value of cohesive energy also exhibits a similar trend.

The phase transition pressures of K-As compounds are calculated from the Gibbs free energy at 0 K. The value of phase transition pressure is obtained from the same eos data where the phase transition occurs once the enthalpy difference of the two phases becomes zero (see Figs. 3, 4). It is well-know that the interatomic and intermolecular distances of crystal change with increased hydrostatic pressure. The shape and orientation of structure under very small displacement of atoms in crystal becomes distorted. So, the phase transition causes reconstruction of the initial structure [29].



**Fig. 4** Volume versus pressure curves of K$_3$As compound in Na$_3$As and Li$_3$Bi phases (Same method is used for the other transitions)
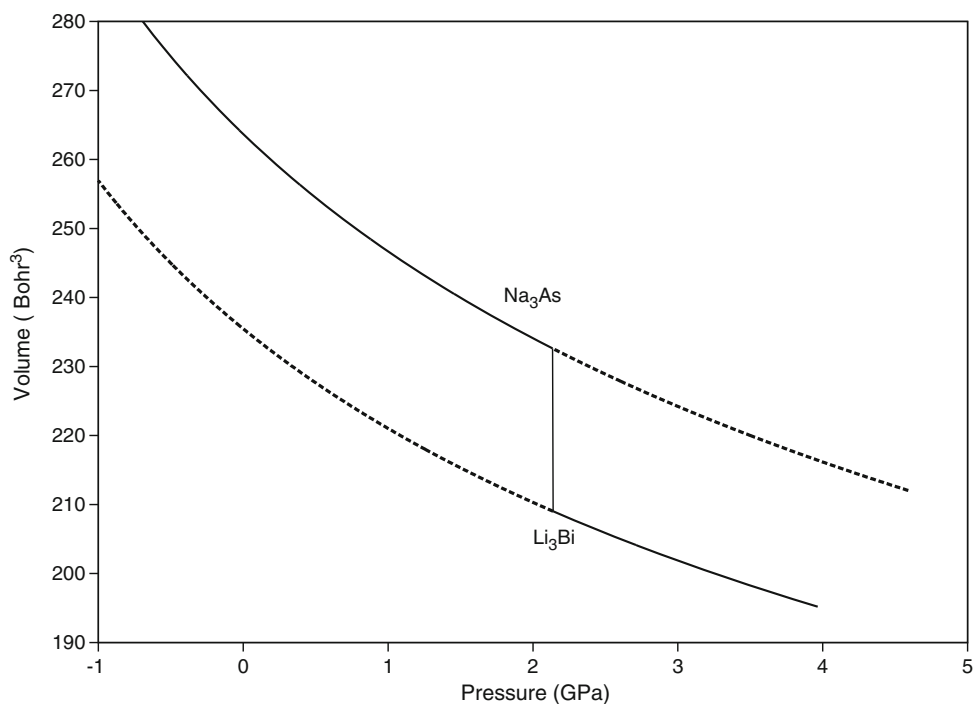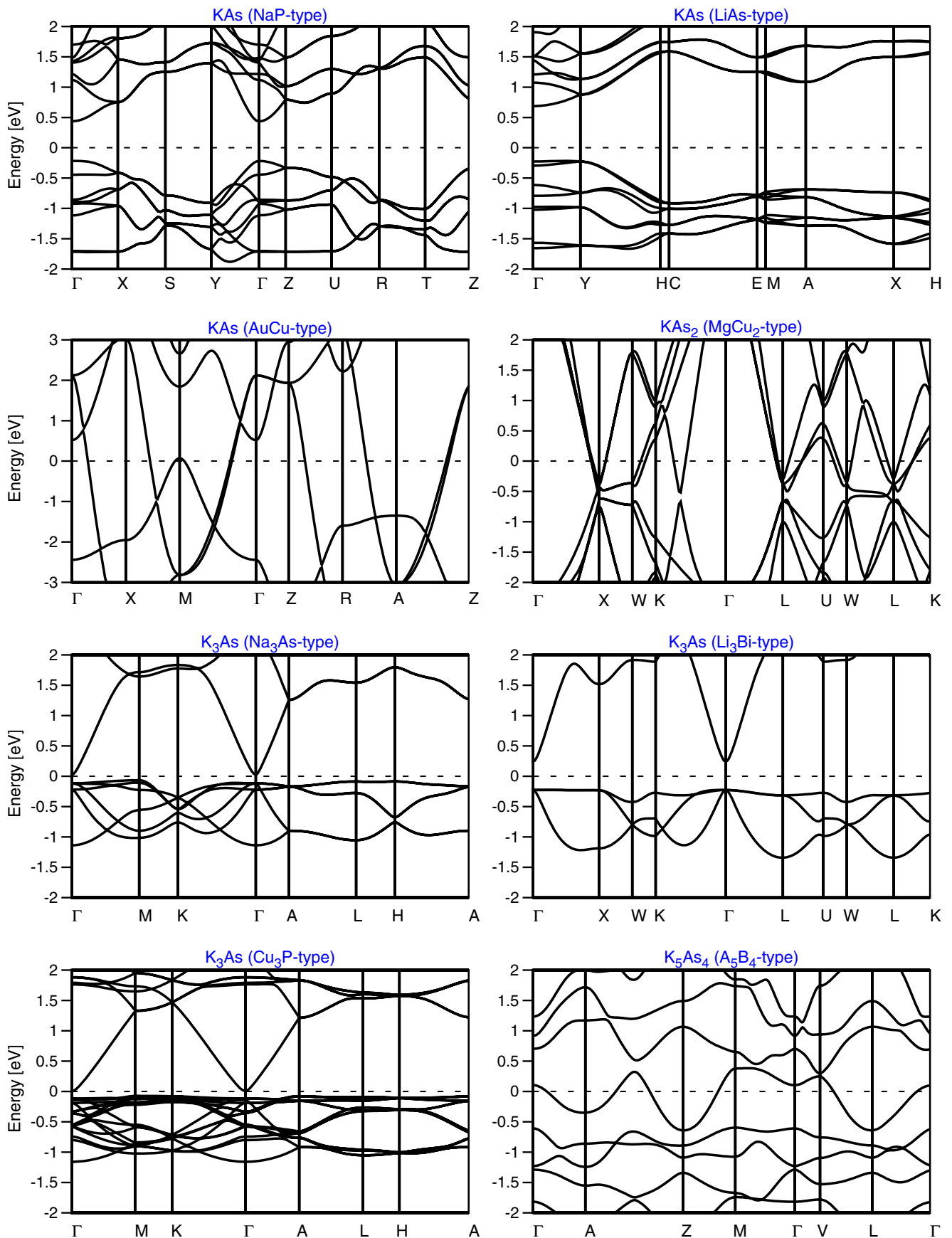
Fig. 5 The calculated band structures of K-As compounds along the high symmetry directions

In this context, the phase transition pressure from NaP to LiAs (AuCu) phase and from LiAs to AuCu phase are found to be 0.8 (10.1) and 11.1 GPa with a 1.7% (19.5%) and 17.2% volume collapse, respectively. Also, the phase transition pressure from $Cu_3P$ ($Na_3As$) to $Li_3Bi$ phase is found to be 2.2 GPa (2.1 GPa) with a 10.1% (10.1%) volume collapse. These trends are very similar to that of Na-As [30].

We have also calculated the band structures of K-As compounds along the high symmetry directions by using

the calculated equilibrium lattice parameters. No other experimental or theoretical data seem to exist to compare with the present results. It can be seen from Fig. 5 that 0.654, and 0.468 eV direct band gap exists at Γ point for NaP and $Li_3Bi$ phases, respectively, and 0.904, 0.092, and 0.080 eV indirect band gap exists from Γ-Y to Γ, from M to Γ, and from M to Γ for LiAs, and $Na_3As$ and $Cu_3P$ phases, respectively. NaP, LiAs, and $Li_3Bi$ exhibit semiconductor character and AuCu, $MgCu_2$, and $A_5B_4$ phases exhibit metallic character. The



**Fig. 6** The calculated partial density of states of KAs in NaP, LiAs, and AuCu phases, respectively (Vertical axis is density (states/eV) in arbitrary unit)
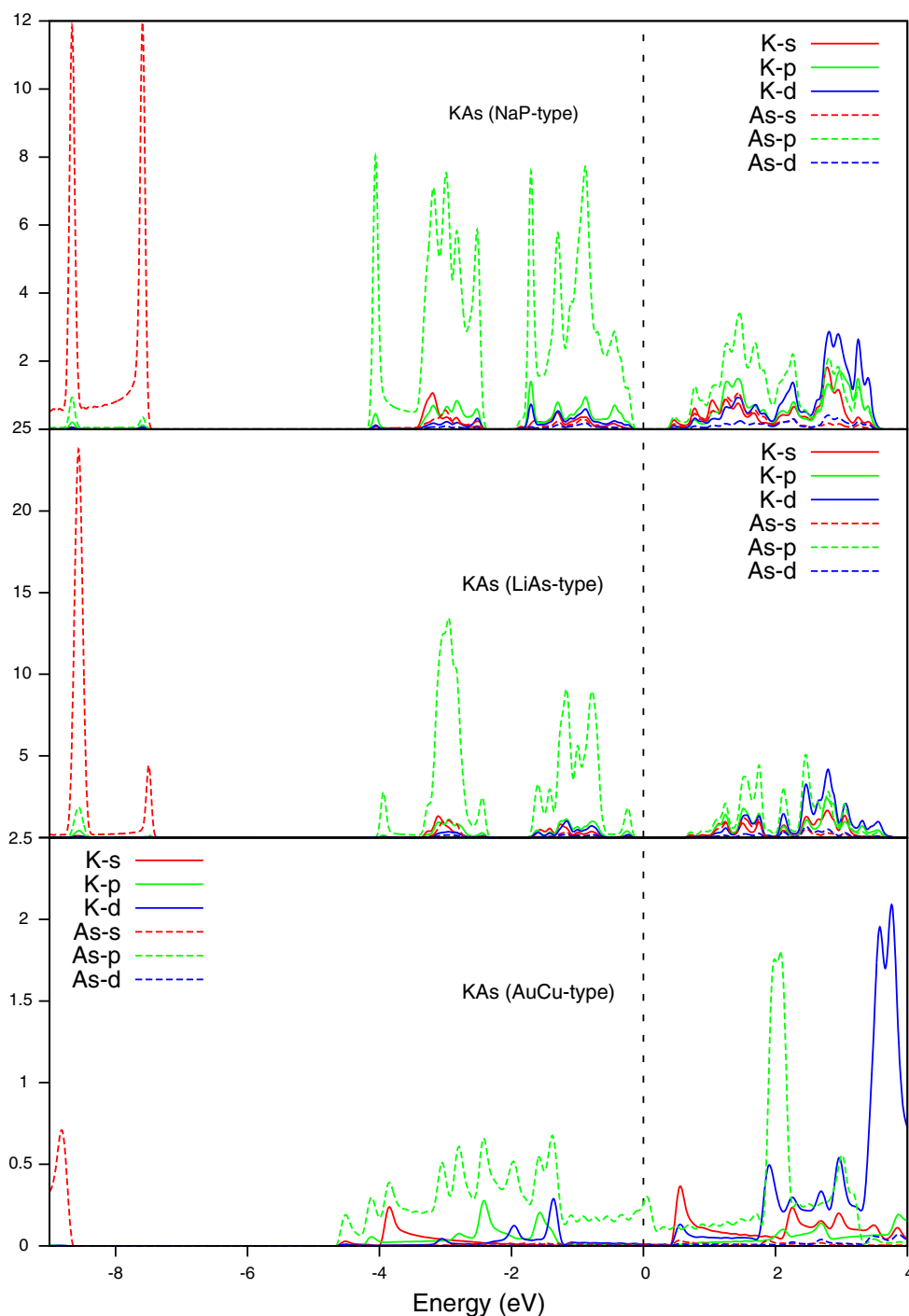
highest value of band gap (0.904 eV) for K-As compounds is found for LiAs phase as in the case of Na-As (1.013 eV) [30], and the trend of band gap is similar to that of Na-As compounds except for $Li_3Bi$ phase [30]. $Na_3As$ and $Cu_3P$ phases have semiconductor character with very narrow band gap. It is known that the narrow band gap materials are important for mid-infrared optoelectronic applications [31–33]. In this context, these compounds may be viable alternatives for infrared applications.

The partial density of states (PDOS) corresponding to the band structures shown in Fig. 5 is also calculated and the obtained result are indicated in Figs. 6, 7, and 8. The position of the Fermi level is set to 0 eV. In Fig. 6, for NaP phase the lowest valence bands occur about -8.5 and -7.5 eV and are essentially dominated by As-s states. The other valence bands are dominated by As-p states, with a minor presence in other energetically degenerate states. The conduction band edge consists essentially of As-p states. K-



Fig. 7 The calculated partial density of states of $K_3As$ in $Na_3As$, $Li_3Bi$, and $Cu_3P$ phases, respectively (Vertical axis is density (states/eV) in arbitrary unit)
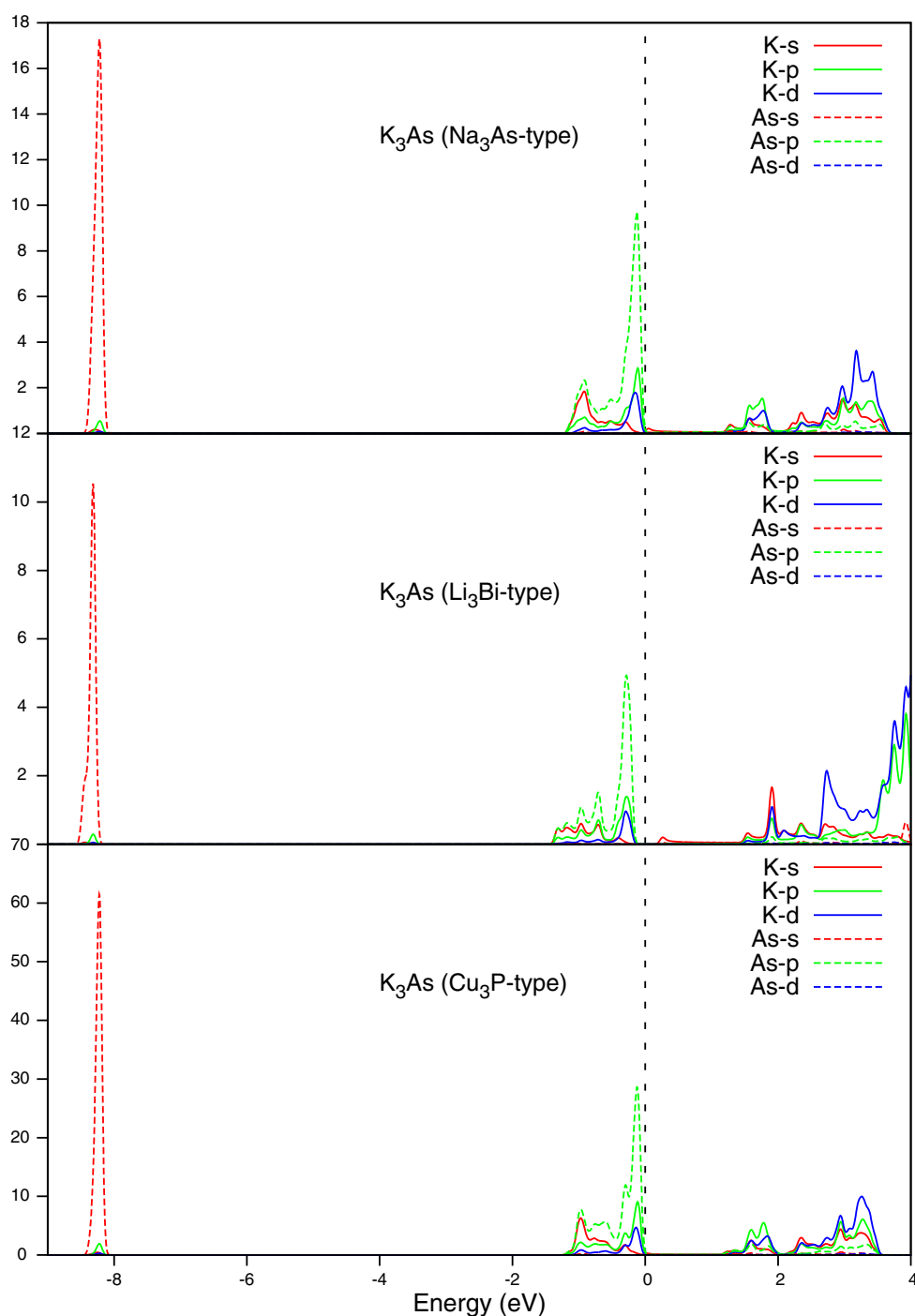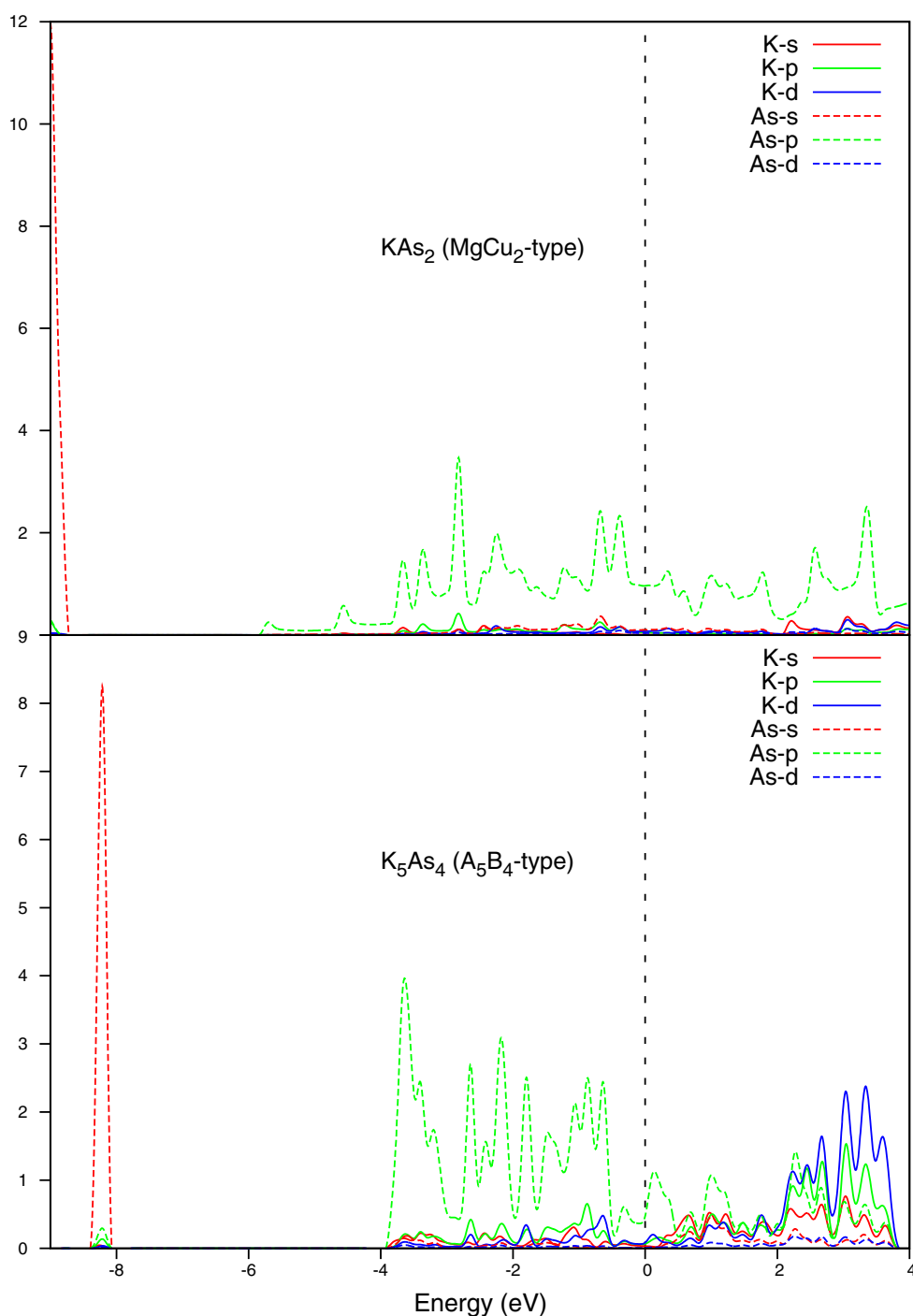
d states dominated above 3.5 eV and the others are energetically degenerate. LiAs phase is similar to the NaP phase. For AuCu phase, the lowest valence bands occur above -8.5 eV and are essentially dominated by As-s states. The other valence bands are essentially dominated by As-p states. In the conduction band, maximum density of states arise at about 2 eV and 3.5 eV by As-p and K-d, respectively. In Fig. 7, the lowest valence band takes place at about -8.2 eV and are essentially dominated by As-s states for all compounds. The other valence bands are essentially dominated by As-p states and the conduction bands are dominated K-s-p and d states. In Fig. 8, lowest valence bands of MgCu$_2$ occur at about -9 eV and are dominated As-s states. The other valence bands and conduction bands are dominated As-p states. For A$_5$B$_4$, As-s states are occur about at -8.2 eV and the other valence bands and are dominated As-p states. The conduction bands between 0 and 1.3 eV are dominated As-p. Above 2 eV K-d states are dominated and K-p-s and As-p states are degenerated, these results imply that the possibility of covalent bonding

between K and As atoms. The states close to the Fermi level are essentially dominated As-p states which give rise to the electrical conductivity for $MgCu_2$ and $A_5B_4$.

Elastic properties

The elastic constants of solids provide a link between the mechanical and dynamical behavior of crystals, and give important information concerning the nature of the forces operating in solids. In particular, they provide information on the stability and stiffness of materials, and their *ab initio* calculation requires precise methods. Since the forces and the elastic constants are functions of the first-order and second-order derivatives of the potentials, their calculation will provide a further check on the accuracy of the calculation of forces in solids. The present elastic constants are computed by using the "stress–strain" method [34], and the results are listed in Table 3. For the stability of lattice, the traditional Born's stability criteria's should be satisfied. Single-crystalline elastic moduli and mechanical stability criteria for the considered structures (Cubic, hexagonal, tetragonal, orthorhombic, and monoclinic) are given in Refs. [35, 36]. It is known that the Voigt bound is obtained by the average polycrystalline moduli based on an assumption of uniform strain throughout a polycrystal and is the upper limit of the actual effective moduli while the Reuss bound is obtained by assuming a uniform stress and is the lower limit of the actual effective moduli [36].

The bulk modulus ($B$), shear modulus ($G$), Young's modulus ($E$), and Poisson's ratio ($\nu$), which are the most interesting elastic properties for applications, are often measured for polycrystalline materials when investigating their hardness. We use the Hill average [37] to calculate Young's modulus ($E$) and Poisson's ratio ($\nu$) using the common relations [38, 39].

The calculated elastic constants are given in Table 3. Our results show that K-As compounds are mechanically stable except for AuCu phase at 0 K and 0 GPa conditions. The elastic constants $C_{11}$, $C_{22}$ and $C_{33}$ measure the *a*-, *b*- and *c*-direction resistance to linear compression, respectively. $C_{33}$

is higher than the $C_{11}$ and $C_{22}$ for $A_5B_4$ structure, so c-axis is less compressible than the other axes for this structure. The highest value of $C_{44}$ is found for $MgCu_2$ phase, and it implies more resisting for monoclinic shear distortion in (100) plane.

The calculated bulk modulus, isotropic shear modulus, Young's modulus and Poisson's ratio are given in Table 4. It is known that isotropic shear modulus and bulk modulus are a measure of the hardness of a solid. The bulk modulus is a measure of resistance to volume change by applied pressure, whereas the shear modulus is a measure of resistance to reversible deformations upon shear stress [40]. Therefore, isotropic shear modulus is a better predictor of hardness than the bulk modulus. The calculated bulk modulus from the eos and elastic constants is almost the same (see Tables 2 and 4). The shear modulus for $MgCu_2$ phase is higher than the other ones, and the trend is similar to the Na-As compounds [30].

Young's modulus is defined as the ratio of the tensile stress to the corresponding tensile strain and it is a measure of the stiffness of the solid. The material is stiffer if the value of Young's modulus is high. Here, the highest value of Young's modulus (78.2 GPa) is found for $MgCu_2$ phase, and it is stiffer than the other phases, and these phases possess almost a soft character.

The value of Poisson's ratio is indicative of the degree of directionality of covalent bonds. The typical value of Poisson's ratio is about 0.1 for covalent materials and 0.25 for ionic materials [41]. The present value of the Poisson's ratio is close to 0.25, therefore the ionic contributions to the interatomic bonding are dominant for these compounds.

Poisson's ratio also, provides more information dealing with the characteristic of the bonding forces than any of the other elastic constants; 0.25 and 0.5 are the lower and upper limits for central force solids, respectively [42]. Inter-atomic forces are predominantly central forces for some phases (NaP, LiAs, $Na_3As$, $Li_3Bi$, and, $Cu_3P$) than the other ones ($MgCu_2$, and $A_5B_4$ phases).

According to the criterion [43, 44], a material is brittle (ductility) if the B/G ratio is less (high) than 1.75. Therefore, these compounds are classified as brittle in nature except

**Table 3** The calculated elastic constants ($C_{ij}$, in GPa) of K-As compounds in considered phases

| Compound | Prototype | $C_{11}$ | $C_{12}$ | $C_{13}$ | $C_{15}$ | $C_{22}$ | $C_{23}$ | $C_{25}$ | $C_{33}$ | $C_{35}$ | $C_{44}$ | $C_{46}$ | $C_{55}$ | $C_{66}$ |
|---|---|---|---|---|---|---|---|---|---|---|---|---|---|---|
| KAs | NaP | 38.2 | 19.0 | 12.9 | | 42.8 | 20.3 | | 43.0 | | 20.5 | | 15.2 | 18.0 |
| KAs | LiAs | 40.2 | 19.8 | 14.4 | -6.3 | 43.9 | 19.3 | -0.6 | 42.2 | 3.5 | 19.2 | -0.4 | 16.5 | 19.2 |
| KAs | AuCu | 54.6 | 11.5 | 13.4 | | | | | 95.7 | | 25.3 | | | -24.4 |
| $KAs_2$ | $MgCu_2$ | 86.3 | 24.6 | | | | | | | | 33.5 | | | |
| $K_3As$ | $Na_3As$ | 26.1 | 8.8 | 4.9 | | | | | 28.6 | | 5.5 | | | 8.6 |
| $K_3As$ | $Li_3Bi$ | 16.6 | 12.6 | | | | | | | | 14.0 | | | |
| $K_3As$ | $Cu_3P$ | 25.5 | 8.6 | 5.6 | | | | | 26.8 | | 6.1 | | | 8.5 |
| $K_5As_4$ | $A_5B_4$ | 34.7 | 11.9 | 10.6 | -1.6 | 37.2 | 8.1 | 0.7 | 72.5 | 6.0 | 13.7 | 0.6 | 13.6 | 14.0 |

**Table 4** The calculated Bulk modulus (B in GPa), Young's modulus (E in GPa), Shear modulus (G in GPa), Poisson ratio ($\nu$), Debye temperature ($\Theta_D$ in K°), and sound velocities ($v_l$, $v_t$, $v_m$ in m/s) of considered phases of K-As compounds

| Compound | Prototype | B | G | E | $\nu$ | B/G | $\theta_D$ | $v_l$ | $v_t$ | $v_m$ |
|---|---|---|---|---|---|---|---|---|---|---|
| KAs | NaP | 25.1 | 15.0 | 37.5 | 0.2508 | 1.673 | 235.8 | 3972 | 2291 | 2544 |
| KAs | LiAs | 25.8 | 14.9 | 37.5 | 0.2571 | 1.725 | 234.8 | 3963 | 2266 | 2518 |
| $KAs_2$ | $MgCu_2$ | 45.1 | 32.3 | 78.2 | 0.2109 | 1.396 | 311.3 | 4530 | 2741 | 3030 |
| $K_3As$ | $Na_3As$ | 13.1 | 7.7 | 19.3 | 0.2542 | 1.701 | 189.2 | 3382 | 1941 | 2156 |
| $K_3As$ | $Li_3Bi$ | 13.9 | 6.6 | 17.0 | 0.2950 | 2.106 | 172.8 | 3151 | 1699 | 1897 |
| $K_3As$ | $Cu_3P$ | 13.0 | 7.8 | 19.5 | 0.2500 | 1.666 | 190.4 | 3385 | 1954 | 2170 |
| $K_5As_4$ | $A_5B_4$ | 22.0 | 15.0 | 36.7 | 0.2217 | 1.463 | 240.3 | 3946 | 2359 | 2611 |

$Li_3Bi$ phase. Moreover, for covalent and ionic materials the typical relations between bulk and shear moduli are $G \approx 1.1B$ and $G \approx 0.8B$, respectively [41]. Here, the G/B ratio for all compounds strongly supports the ionic contribution to interatomic bonding.

As an important fundamental parameter, the Debye temperature ($\Theta_D$) is closely related to many physical properties of solids such as the specific heat and melting temperature. At low temperatures the vibrational excitations arise solely from acoustic vibrations. Hence, at low temperatures the Debye temperature calculated from elastic constants is the same as that determined from specific heat measurements. One of the standard methods for calculating the Debye temperature is to use elastic constant data since $\Theta_D$ may be estimated from the average sound velocity ($v_m$) [45, 46].

The calculated Debye temperatures are listed in Table 4 for studied phases. The lowest value of Debye temperature is found for the $Li_3Bi$ phase as in the case of the Na-As compounds in our recent work [30]. Generally, the Debye temperature for soft (hard) materials is lower (higher) [47]. This compound with various stochiometries possesses the low Debye temperature, so again it is a soft material.

The elastic anisotropy of crystals affects the physical properties in different directions of solids, e.g., cracks and dislocations can be induced by elastic anisotropy [48]. The shear anisotropic factors are a measure of the degree of anisotropy in the bonding between atoms in different planes. For an isotropic crystal, the values of $A_1$, $A_2$ and $A_3$ equal to 1 and any value smaller or greater than 1 is a measure of the degree of shear anisotropy. The shear anisotropy factors are given as $A_1 = 4\,C_{44}/(C_{11}+C_{33}-2\,C_{13})$ for the {100} shear planes between <011> and <010> directions, $A_2 = 4\,C_{55}/(C_{22}+C_{33}-2\,C_{23})$ for the {010} shear planes between <101> and <001> directions, and similarly, for the {001} shear planes between <110> and <010> directions and it is $A_3 = 4\,C_{44}/(C_{11}+C_{22}-2\,C_{12})$. The shear anisotropy factors are given as $A_1=A_2=A_3$, and $A_1=A_2$ for cubic, and hexagonal structure, respectively. In addition, we have also calculated the percentage elastic anisotropy for polycrystalline materials which is defined as $A_B=(B_V-B_R)/(B_V+B_R)$ and $A_G=(G_V-G_R)/(G_V+G_R)$ in compressibility and shear, respectively. Where the subscripts V and R represent the Voigt and Reuss approximations, respectively. In these expressions, "the zero value" corresponds to the elastic isotropy and the value of 100% identifies the largest elastic anisotropy.

Our results are tabulated in Table 5 for K-As compounds. $MgCu_2$ is elastically isotropic and, relatively, has low percentage of anisotropy in compression and shear. $Na_3As$ and $Cu_3P$ phases are elastically isotropic for the {001} shear planes and the elastically anisotropic for the {100}({010}) shear planes. $Li_3Bi$ possesses the highest anisotropy and percentage of anisotropy in shear among all phases considered.

**Table 5** The calculated shear anisotropic factors ($A_1$, $A_2$, and $A_3$) and the percentage of anisotropy in the compression and shear ($A_B$ and $A_G$)

| Compound | Prototype | $A_1$ | $A_2$ | $A_3$ | $A_B$ (%) | $A_G$ (%) |
|---|---|---|---|---|---|---|
| KAs | NaP | 1.480 | 1.345 | 1.674 | 0.749 | 3.163 |
| KAs | LiAs | 1.432 | 1.391 | 1.731 | 0.646 | 5.987 |
| $KAs_2$ | $MgCu_2$ | 1.086 | | | 0 | 0.155 |
| $K_3As$ | $Na_3As$ | 0.490 | | 0.994 | -0.019 | 4.501 |
| $K_3As$ | $Li_3Bi$ | 7 | | | 0 | 38.346 |
| $K_3As$ | $Cu_3P$ | 0.594 | | 1.006 | -0.131 | 2.434 |
| $K_5As_4$ | $A_5B_4$ | 0.637 | 0.583 | 1.169 | 3.875 | 5.382 |

## Conclusions

In conclusion, by performing first-principles calculations, we have studied the structural, mechanical and electronic properties of K-As compounds. The calculated lattice parameters are in agreement with the available experimental data. The phase transition from NaP to LiAs (AuCu) phase, from LiAs to AuCu phase and from $Cu_3P$ ($Na_3As$) to $Li_3Bi$ phase are found to be 0.8 (10.1), 11.1, and 2.2 (2.1) GPa with 1.7% (19.5%), 17.2% and 10.1% (10.1%) volume collapse, respectively. NaP, LiAs, $Na_3As$, $Li_3Bi$, and $Cu_3P$ phases exhibit the semiconductor character, while the AuCu, $MgCu_2$, and $A_5B_4$ phases are metallic in nature. The other original aspects of the present calculations concern the elastic and mechanical results, which were not considered previously. The considered phases of KAs, except AuCu phase, are mechanically stable. The calculated values of the shear modulus, Young modulus, Debye temperature and elastic wave velocities are highest for $MgCu_2$ phase. Moreover, this compound with various stoichiometries has ionic character and the $Li_3Bi$ phase can be classified as ductile with higher anisotropy, and the other phases are brittle in nature. Consequently, we conclude that our theoretical predictions on the considered properties of these compounds would serve as a reliable reference for further experimental and theoretical investigations in the future.

## References

1. Xu WG, Jin B (2006) J Mol Struc THEOCHEM 759:101–107
2. Burtzlaff S, Holynska M, Dehnen S (2010) Z Anorg Allg Chem 636:1691–1693
3. Tegze M, Hafner J (1992) J Phys Condens Matter 4:2449–2474
4. Derrien G, Tillard M, Manteghetti A, Belin C (2003) Z Anorg Allg Chem 629:1601–1609
5. Ettema ARHF, de Groot RA (1999) J Phys Condens Matter 11:759–766
6. Hirt H, Deiseroth H (2004) Z Anorg Allg Chem 630:1357–1359
7. Yan J-Q, Nandi S, Zarestky JL, Tian W, Kreyssig A, Jensen B, Kracher A, Dennis KW, McQueeney RJ, Goldman AI, McCallum RW, Lograsso TA (2009) Appl Phys Lett 95:222504
8. Chen ZG, Yuan RH, Dong T, Wang NL (2010) Phys Rev B 81:100502
9. Dong T, Chen ZG, Yuan RH, Hu BF, Cheng B, Wang NL (2010) Phys Rev B 82:054522
10. Sangster J, Pelton AD (1993) J Phase Equilib Diff 14:240–242
11. Brauer G, Zintl E (1937) Z Phys Chem B 37:323–352
12. Mansmann M (1965) Z Kristallogr 122:399–406
13. Emmerling F, Röhr C (2002) Z Naturforsch Sec B - Journal Chem Sc 57:963–975
14. Gascoin F, Sevov SC (2001) Inorg Chem 40:5177–5181
15. Hönle W, Buresch J, Peters K, Chang JH, von Schnering HG (2002) Z Kristallogr - New Cryst Struct 217:483–484
16. Emmerling F (2003) Pnictide und Oxopnictate der schweren Alkalimetalle — Darstellung, Charakterisierung und Kristallchemie. Albert-Ludwigs-Universitat, PhD Thesis, Breisgau
17. Voronin GF, Bludova LN (1974) Vestnik Belorusskogo Gosudarstvennogo Universiteta Seriya 2 Khimiya Biologiya Geografiya 15:433-435
18. Dorn FW, Klemm W, Lohmeyer S (1961) Z Anorg Allg Chem 309:204–209
19. Sieberer M, Redinger J, Khmelevskyi S, Mohn P (2006) Phys Rev B 73:1–9
20. Gao GY, Yao KL, Liu ZL, Min Y, Zhang J, Fan SW, Zhang DH (2009) J Phys Condens Mater 21:275502
21. Kresse G, Hafner J (1994) Phys Rev B 47:558–561
22. Kresse G, Joubert D (1999) Phys Rev B 59:1758–1775
23. Kresse G, Furthmuller J (1996) Comput Mater Sci 6:15–50
24. Kresse G, Furthmuller J (1996) Phys Rev B 54:11169–11186
25. Perdew JP, Burke K, Ernzerhof M (1996) Phys Rev Lett 77:3865–3868
26. Blöchl PE (1994) Phys Rev B 50:17953–17979
27. Murnaghan FD (1937) Am J Math 49:235–260
28. Maradudin AA, Montroll EW, Weiss GH, Ipatova IP (1971) Theory of lattice dynamics in the harmonic approximation. Academic, New York
29. Chandra Shekar NV, Govinda Rajan K (2001) Bull Mater Sci 24:1–21
30. Ozisik HB, Colakoglu K, Deligoz E, Ozisik H (2011) Solid State Commun 151:1349–1354
31. Meyer JR, Olafsen LJ, Aifer EH, Bewley WW, Felix CL, Vurgaftman I, Yang MJ, Goldberg L, Zhang D, Lin C-H, Pei SS, Chow DH (1998) IEE Proc Optoelectron 145:275–280
32. McGill TC, Collins DA (1993) Semicond Sci Technol 8:S1–S5
33. Krishnamurthy S, Chen AB, Sher A (1996) J Appl Phys 80:4045–4048
34. Page YL, Saxe P (2001) Phys Rev B 63:174103
35. Ozisik H, Colakoglu K, Ozisik HB, Deligoz E (2010) Comput Mater Sci 50:349–355
36. Wu Z, Zhao E, Xiang H, Hao X, Liu X, Meng J (2007) Phys Rev B 76:054115
37. Hill R (1952) Proc Phys Soc A 65:349–354
38. Voigt W (1928) Lehrburch der Kristallphysik. Teubner, Leipzig
39. Reuss A (1929) Z Angew Math Mech 9:49–58
40. Florez M, Recio JM, Francisco E, Blanco MA, Penda's AM (2002) Phys Rev B 66:144112
41. Bannikov VV, Shein IR, Ivanovskii AL (2008) Phys Status Solidi-R 1:89–91
42. Fu H, Li D, Peng F, Gao T, Cheng X (2008) Comput Mater Sci 44:774–778
43. Pugh SF (1954) Philos Mag 7(45):823–843
44. Shein IR, Ivanovskii AL (2008) J Phys Condens Mater 20:415218
45. Johnston L, Keeler G, Rollins R, Spicklemire S (1996) Solid state physics simulations. The consortium for upper-level physics software. Wiley, New York
46. Schreiber E, Anderson OL, Soga N (1973) Elastic constants and their measurements. McGraw-Hill, New York
47. Zhao E, Wang J, Wu Z (2010) J Comput Chem 31:2883–2888
48. Miao N, Sa B, Zhou J, Sun Z (2011) Comput Mater Sci 50:1559–1566